

# Design and Control of Distributed Generations (DGs) for Microgrid Applications

Yam Krishna Poudel <sup>a</sup>, Nava Raj Karki <sup>b</sup>, Netra Prasad Gyawali <sup>c</sup>, Dayasagar Niraula <sup>d</sup>

<sup>a, b, c</sup> Institute of Engineering, Pulchowk Campus, Tribhuvan University, Nepal

<sup>d</sup> Nepal Engineering College, Changunarayan, Bhaktapur, Nepal

✉ <sup>a</sup> yampdl01@gmail.com, <sup>b</sup> nrkarki@ioe.edu.np, <sup>c</sup> netra@ioe.edu.np, <sup>d</sup> dayasagar2733@gmail.com

## Abstract

Climate change has a significant influence on the environment, and the scarcity of natural resources necessitates scientific research and innovative technical solutions. This research aims to develop scientific and technological approaches to green technologies, that are ecologically beneficial and sustainable where energy and power supplies are major concerns. This study focuses on design and control of distributed generations for microgrid applications. Microgrids are designed to operate in both modes, albeit primarily focused on the isolated mode, which includes Solar Photovoltaics, Wind energy, and Battery Storage Units. For solar and wind energy, maximum power point tracking (MPPT) is used to extract the maximum power output from these sources. The Voltage Source Inverter (VSI)-based inverter enables nearby household energy production to actively deliver electricity to the utility grid while operating in standalone mode and keeping power quality criteria. Electrical parameters of the battery are modelled and different distributed generations were finally optimized and the developed model is simulated and analyzed in MATLAB for maintaining and synchronizing power quality and frequency with the aid of novel control approach. Synchronous reference frame (d-q) theory is used for control algorithm where inner current control and outer current control (dual mode) is used for the efficient control. Particle Swarm Optimization (PSO) is used for optimization of PID. Grid formation and grid feeding conditions of microgrids are analyzed, discussed and presented. The results elucidate the satisfactory operation of the system under variations both on the generations and consumptions. This research has a great impact in micro grid development process as the microgrids contain multiple DGs and operate in islanding mode. This research completes the design of DC microgrid which is able to operate in both grid feeding and grid forming mode.

## Keywords

Distributed Generations (DGs), Maximum Power Point (MPP), Microgrid, Particle Swarm Optimization, Synchronous Reference Frame

## 1. Introduction

The recent Java blackout, which occurred from August 4-5, 2019 affected about twelve crores people in Indonesia. A massive blackout happened in 2012 in India that impacted about 62 crores to 70 crores people i.e. about almost half of India's population (10% of global population). In the current scenario, many countries have experienced blackouts that causes direct impact on millions of people and ecosystem of business. Overdrawing of grid electricity, technical failures of transmission lines, transformers, generator malfunctioning) human(operator)mistake, harsh weather conditions, and natural disasters are the major causes that can cause the issue of blackout. Only a few (one or two) major events are often responsible for these huge outages. A single power system failure can throw modern society into disarray. When power plants must be brought back up after a wide-ranging blackout, restoring power (resiliency) can be difficult [1]. Airports and major companies, were unaffected because backup generators were available during India's 2012 blackouts. For hospitals, academic institutions, and skyscrapers, standard distributed generation (DG) backup generators have been widely used as emergency and standby generation. Many researchers have recently turned their attention to the concept of decentralization of power systems with green and clean energy as a result of growing worries about traditional fossil energy shortages and

other environmental challenges appearing in recent years that can continue in future. As a result, power systems have undergone significant changes, not only to ensure sustainable development but also to make significant breakthroughs in solving power problems in remote areas. One such notable innovation is the micro-grid (MG), which can integrate various types of energy sources and power electronics interfaced with distributed generation (DG) and renewable energy sources (RES) [2].

## 2. Literature review

### 2.1 Distributed Generation

Distributed generation, as described by IEEE [3], is the production of electricity by establishments that are sufficiently smaller than central generating plants to permit connectivity practically at any point in the power system. They are theoretically smaller than centralized systems. DG is usually placed close to loads to avoid transmission losses. DG does not replace conventional centralized generation, but it does offer a reliable, highly efficient, and economically viable way to supply enough electricity to load centers. There is a limited prospect of installation of new transmission lines due to land limits, popular will, and environmental damage. Because of this, even though there is enough power capacity, it is challenging to meet the load

center's peak power requirements. By putting DG at the top of the priority list, power demand can be met locally if there is a nearby load center. Different generation configurations are represented by the letters DG and CG. Almost thirty years ago, centralized production seemed unassailable due to the fact that the cost savings from larger power plants outweighed the greater costs of transporting energy to the users, and DG was practically nonexistent in the 1960s. Because of the inherent advantage of affordable transportation and the use of renewable energy, the dependence on fossil fuels and their prices may be decreased. The decrease of carbon dioxide emissions as a result of this action is considerable [4]. Co-generation or Combined Heat and Power (CHP) plants use one process to generate both heat and electricity. Waste heat from the generation process might be used to industrial processes or used to provide heat for the neighborhood communities [5]. These applications might increase the system's overall efficiency by a factor of four [6]. In DG, several prime movers are employed, including IC engines, microturbines, solar and wind turbines, fuel cells, and others. The main energy producers that need inverters to connect to the distribution networks are microturbines, solar panels, and fuel cells [7]. The output voltage and frequency are made compatible with the electrical grid by the power electronics-based inverters. The inverter will not produce a perfect sinusoidal wave of alternating current (AC). When Direct Current (DC) is changed to Alternating Current (AC), occasionally strong harmonics can be created [7]. Harmonic distortion must be kept within allowable industrial ranges. Variations in voltage and frequency may be deteriorated by the irregular power produced by renewable energy sources. Several apps fail when DG is used alone.

## 2.2 From Distributed Generation to Microgrid

For distributed generations, a range of technological challenges related to managing several micro sources are of essential significance [8]. It is possible for individual distributed generators to create as many problems as they can create [9] [10]. Realizing the potential of DG requires a systematic strategy that integrates the generating and related loads in a given region as one subsystem or microgrid [10]. This considerably raises power system's reliability [11]. Microgrids are collections of electrical generation, storage, and loads that can run concurrently with or separately from the main grid [12] [13]. To put it another way, a microgrid generator's output may be changed from zero to its rated power. The generators at a conventional power plant are expected to continue working. Microgrids can be isolated or linked to the grid. In microgrids, solar and wind power systems are both regarded as types of variable (non-deterministic) generators. The weather has a big impact on them. An Internal Combustion (IC) engine powers a regulated (deterministic) generator. The tiny size of the generators used in microgrids allows for their ability to be turned on and off for the improvement of the frequency of operation recalls for a specific facility [14] [15]. The interconnection switch links the microgrid to the remaining distribution network at the Point of Common Coupling (PCC). Renewable energy may be used in the microgrid without extra frequency management due to the utility grid's connection to it. Utility consumers and users of microgrids may also be provided with auxiliary services. Microgrids close to power demand

centers may supply these services considerably more effectively than far-off producing stations since they operate close to the loads [16]. The electrical and thermal demands can both be supported by microgrids. Because the frequency is unconnected to the electrical grid, controlling a microgrid in islanded mode is more fascinating and difficult. When there is a lot of demand variability or when there is a lot of renewable energy, microgrid frequency management might be challenging to accomplish. The microgrid's loads may be isolated from the outage during outages by separating the generating and related loads from the distribution network without affecting the stability of the transmission grid. End users may receive more dependable and high-quality electricity via strategic islanding of generation and loads than from the utility grid [17]. By providing dispatchable electricity at peak times and postponing or avoiding distribution infrastructure improvements, microgrids can also assist the local utility in reducing costs [18]. The smart technologies that have been created and are incorporated into microgrids increase system resilience at the local level. Moreover, microgrids avoid power outages and costs associated with them. Figure ?? shows the microgrid model.

## 2.3 Impact of Microgrids

When distributed generation (DG) is unable to supply all of the electricity needed by the customers, the energy storage components of the distribution system help to maintain the overall system's reliability. Microgrids help with local voltage and frequency management, improve reliability, decrease  $CO_2$  emissions, reduce power losses in the electric distribution network, and increase grid power capacity. One of the novel methods of incorporating distributed generation into the electrical grid is through microgrids. The integration of Distributed Energy Resources (DERs) into microgrids to service a range of loads, such as homes, offices, industrial parks, commercial, and institutional campuses, assists end-users, energy utilities, transmitters, and distributors. Microgrids not only increase consumer reliability, but also improves the security of distribution system and ensures the targeted performance of the system through generation redundancy.

## 3. Microgrid Model Development

### 3.1 Model Development

Hybrid energy systems interconnects renewable production sources such as wind power, photovoltaic power, electric cells, and microturbine generators to provide electricity for local loads or connecting to the grids or microgrids. For getting the maximum power output from the wind and PV array, a large battery bank is required for the load. Because of the development and deployment of renewable DC power sources, as well as the advantages of DC loads in commercial, industrial, and residential applications, DC grids have recently resurged. DC microgrid has been proposed to interface with various distributed generators. AC sources, on the other hand, must be converted to DC before being connected to a DC grid, and standard AC loads require DC/AC inverters. By combining two renewable resources into an ideal combination, the impact of the fluctuating nature of solar and wind resources will be somewhat mitigated, and the whole system will become more reliable and

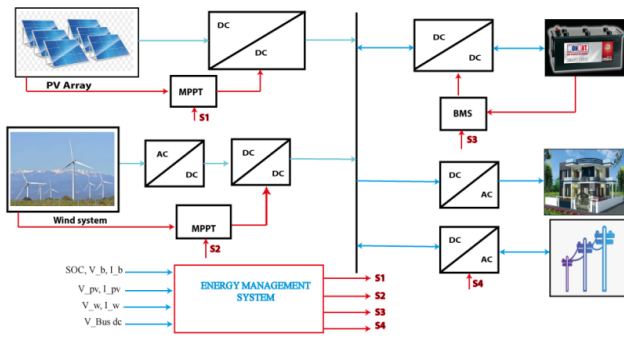


Figure 1: Microgrid Model

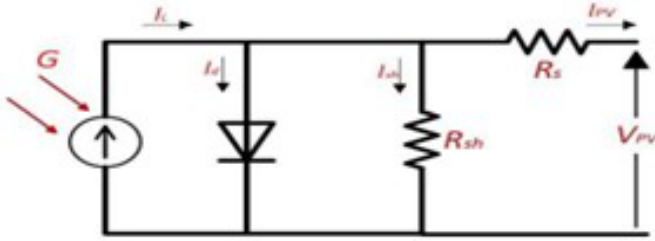


Figure 2: Equivalent circuit of PV cell

cost-effective to operate. There are numerous configurations that present a state-of-the-art review. The developed model for this research consists of solar photovoltaic array, wind and battery storage system connected to DC bus. Inverter is used to connect with the grid and loads. Figure 1 shows the microgrid model.

### 3.2 Modelling of a PV Cell

The solar PV cell, whose structure is depicted in Figure 2, is the most basic component of a photovoltaic system. It is a semiconductor with boron and phosphorus atom added to generate a two-layer p-n junction at high temperatures. Positive and negative ions make up these two layers, which correspond to P-holes and N-electrons, respectively. For an electric current flow, a top electrode and a bottom electrode are added. Finally, an anti-reflective coating is applied to the glass. The photovoltage effect is the primary mechanism used by the cell to convert light into electrical energy. A conventional solar cell does not contain the resistances; nevertheless, for use in real-world scenarios, they are implanted and linked to the PV diode. To figure out the current generator from a solar cell, Kirchhoff's law is utilized.

$$I_{pv} = I_L - I_d - I_{sh} \tag{1}$$

Where  $I_L$  is the current generator.

$$I_L = G\{I(sc)[1 + K(a)(T - T_{stc})]\} \tag{2}$$

where  $G$  is the solar irradiance,  $T$  is the ambient temperature,  $I(sc)$  is the PV cell's short circuit current, and  $K(a)$  is the temperature coefficient  $T_{stc}$  is the PV cell's temperature operation under standard test circumstances (STC), and  $I_d$  is the PV diode's current, as determined by Shockley's equation.

$$I_d = I_o\{\{exp(qV_d)/nkT\} - 1\} \tag{3}$$

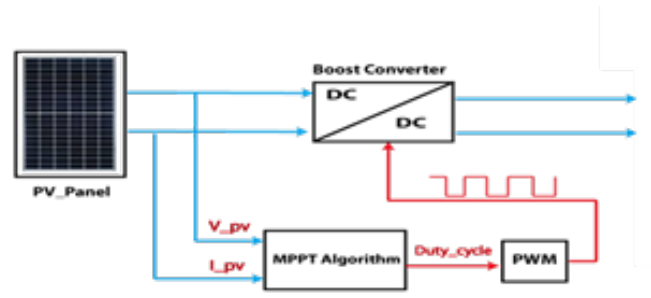


Figure 3: DC-DC Boost converter

Where  $I_o$  is the PV diode's saturation current,  $V_d$  represents the diode voltage,  $q$  represents the electrical charge,  $k$  represents the Boltzmann constant, and  $n$  represents the PV diode factor.

### 3.3 DC-DC Boost Converter

Although other DC-DC converters, such as boost, buck, and chuk converters, have been developed, boost converter is most extensively employed for solar photovoltaic generated systems due to its high efficiency. This is because DC-DC boost converter produces and regulates more output voltage with less output current than the input voltage. According to a loss power equation, the loss power will be modest in this scenario. The MOSFET transistor, on the other hand, is commonly utilized in the construction of DC-DC boost converters because of its capacity to perform under heavy loads and at higher frequencies as well as its lower power losses. When the MOSFET is turned on, current flows in the opposite direction through an inductor, which stores the energy by generating a magnetic field. When the MOSFET transistor is turned off in state two, the energy stored and the primary source are connected in series, resulting in a larger output voltage. As long as the MOSFET switch is open, the inductor current changes linearly. When the MOSFET is turned off, the  $I_L$  rating changes. The overall rating value of the inductor current must be zero to support the steady-state mode of DC-DC converter .

The forward current diode of DC-DC converter should be equivalent to the maximum current load of the PV system.

### 3.4 Control System of a PV System

The photovoltaic array's Maximum Power Point (MPP) is a distinct point on the P-V curve that varies with the weather. The MPPT technology connects the PV array and the load or grid and is used with the PV power conversion system to continuously track the MPP. Duty cycle conversion to signal is accomplished via pulse width modulation (PWM). For the generation of the PWM pulse, the PWM circuit compares the duty cycle signal with a saw-tooth counter signal. In case if the sawtooth signal is smaller than the duty cycle (D)signal, the output PWM signal is said to be in the ON-state ( $T_{on}$ ) else it is considered to be in the OFF-state ( $T_{off}$ ). This operation is repeated to modify the operating work of the PV array under changing weather circumstances. The optimal duty cycle is determined by the operating MPP's position on the P-V curve. The duty cycle will increase till it reaches the MPP when the operating point is to the right, otherwise, it will decrease.

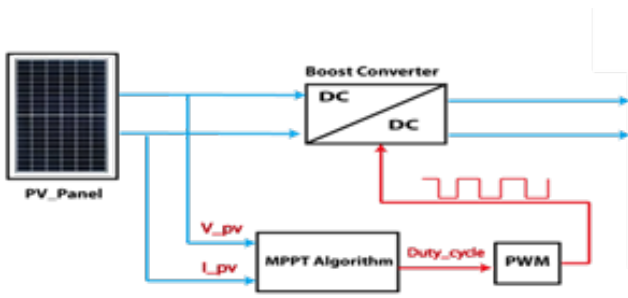


Figure 4: State condition of DC-DC Boost converter

### 3.5 PSO Algorithm

James Kennedy and R.C. Eberhart invented Particle Swarm Optimization (PSO) technique in 1995. It is a stochastic (random variable connection) evolutionary computation approach for exploring search space which is based on the intelligence and movement of swarms. This is a population-based strategy as it is based on swarm behavior. When looking for food, the bird usually takes the shortest route. This algorithm was created based on this behavior. Each particle (of the large number of particles) accelerates in search space based on its understanding of the solution, also by comparing its own best value to that of the swarm. As each particle searches in a certain direction, and by the interaction with the bird and the best location so far, they try to reach that location by modifying their velocity which is properly characterized by the concept of social interaction.

PSO is unaffected by the magnitude of the problem. PSO overcomes the fault of GA, namely premature convergence. As it only has two equations, it is quite simple for practice and application. The equations of PSO algorithm are presented herewith.

$$V_i^{k+1} =$$

$$wv_i^k + c_1 \text{rand}_1 * (pbest_i - s_i^k) + c_2 \text{rand}_2 * (gbest_i - s_i^k)$$

Where,  $v^k$  = velocity of agent  $i$  at iteration  $k$

$w$  = weighing function

The first term,  $wv_i^k$ , refers to the component of inertia that causes a particle to move in the same direction it was before. If the value of 'w' is low, the convergence will speed up; otherwise, exploration will be encouraged. The second term,  $c_1 \text{rand}_1 * (pbest_i - s_i^k)$  represents the cognitive component that acts as memory of the particle. The third term  $c_2 \text{rand}_2 * (gbest_i - s_i^k)$  is the social component, which explains why the particle moves to the best region the swarm has discovered thus far. The position of each particle can be updated using the equation of position modification after the velocity of each particle has been computed.

The proposed flowchart of the algorithm is shown in Figure 5. Because of its low cost and ease of implementation, the PSO algorithm is commonly utilized for PV-MPPT approaches. The main function of this method is to calculate PV power through the use of values of voltage and current values that is sensed from the PV array which are then compared to the previous power to address the direction of the PSO algorithm. The duty cycle (D) of the DC-DC converter is then updated, as needed.

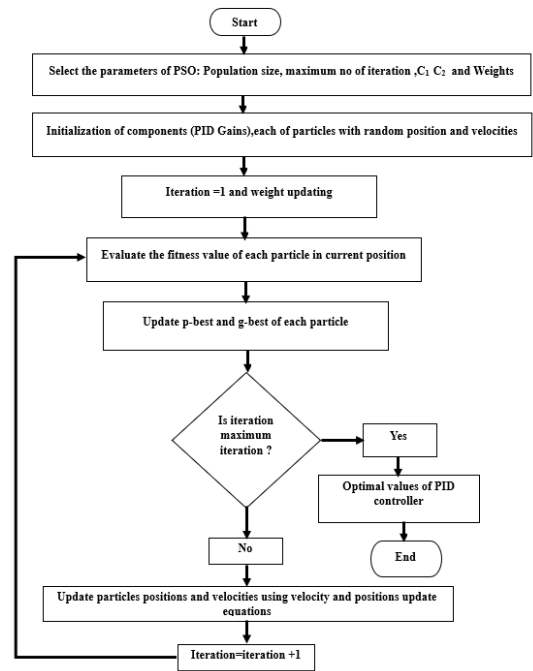


Figure 5: Flowchart of the proposed system

$$D(k+1) = D(k) \pm \Delta D$$

$D(k+1)$  and  $D(k)$  are  $D$ 's next and prior perturbations, respectively, and  $D$  is the reference  $D$ 's incremental step size. If the voltage and power of the PV array rises because of the rising duty cycle, the PSO algorithm's operating point moves in the same direction; otherwise, it travels in the other direction. The cycle is repeated until it reaches the MPP, at which point it oscillates around it. After attaining the MPP, a big duty cycle clearly leads to a quick steady-state and considerable fluctuation of the probabilities of direction for PSO algorithm.

### 3.6 Wind Energy System

Power output of the wind turbine is mathematically denoted as,

$$P = AdV^3/2 \quad (4)$$

where,  $P$  denotes the output power of wind turbine in Watts,  $d$  represents the density of air in  $kg/m^3$ ,  $A$  is swept area in  $m^2$  and  $v$  is Velocity of the wind in m/s.

Betz generalized and examined these parameters and came up with the Betz limit, which is the maximum output power of a wind turbine. This value equals 0.59, which is the maximum power that a wind turbine can produce. Wind turbines today can reach a maximum efficiency of almost fifty percent, which is in line with the restriction. This is how a wind turbine's performance coefficient is calculated. As a result, the wind turbine's output power can be changed into

$$P = kCAv^3/2 \quad (5)$$

At varying wind speeds, the mechanical power of a turbine is plotted as a function of rotor speed. At a set rotor speed, known as the optimum rotor speed, the power for a given wind speed is at its peak. This is the speed that corresponds to the optimal tip speed ratio. In order to get the maximum power out of the



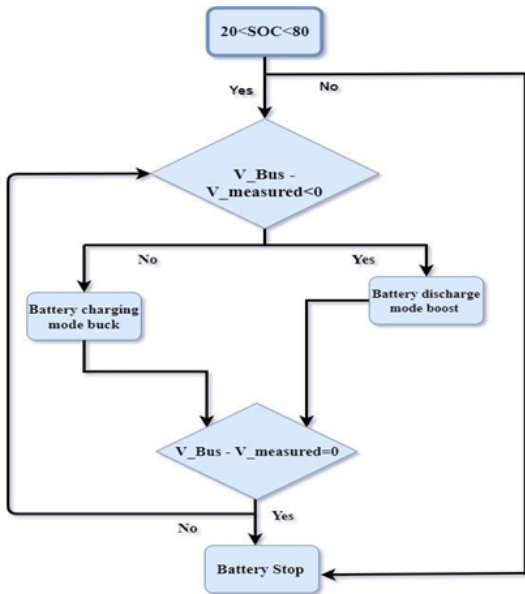


Figure 6: Buck-Boost Battery charging conditions

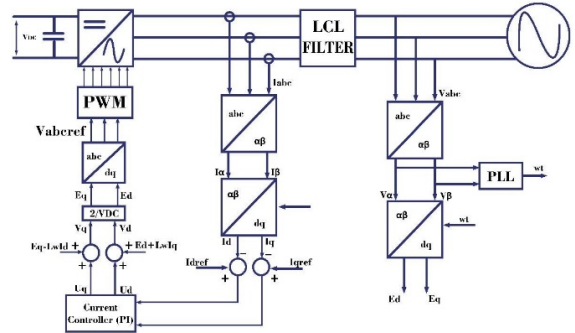


Figure 7: Inverter control for grid connected mode

turbine, it should always be set to optimum. This is accomplished by regulating the turbine’s rotational speed.

### 3.7 Battery Management System

A modified lithium-ion battery model is used. To link the relationship between the battery State of Charge (SOC) and its voltages, ‘H’ factor parameters are used. The characteristics of this type are taken from a battery datasheet. Individual batteries are connected in series or parallel to increase the total storage system voltage or current. As a result, a good battery model is used to build a storage system model.

## 4. Control Methodology

The inverter control is used which includes optimal filtering of LCL output and synchronization of the grid by means of Phase Locked Loop (PLL). PLL feeds the signals to the current loop, which is implemented using a PID controller that can run in grid forming and grid feeding modes. The comprehensive mathematical modeling and description of the LCL filter, as well as a flowchart with the PSO algorithm, are also described and shown. Phase angle of the grid, the grid frequency, and the grid voltage are detected using a PLL algorithm. Frequency and voltage are required for grid monitoring as well as reference frame modifications. The currents are translated into the synchronous frame, and the algorithm additionally achieves the decoupling between two axes, if a PID current control is used.

### 4.1 PLL for Inverter Synchronization with the Utility Grid

Many signal applications and, more recently, power electronics, make extensive use of PLL systems. Several hertz to orders of gigahertz are within the range of frequencies that can be handled by PLL technology. The SRF PLL works well in distorted and imperfect grid environments and can be applied to single-phase and three-phase applications, according to [19]. The phase voltage is obtained, and then the stationary reference frame

voltage is changed into voltages  $V_d$  and  $V_q$  in a frame of reference synchronized to the utility frequency using the  $\alpha$  and  $\beta$  transformations.

### 4.2 DC Bus Voltage Control

DC bus voltage is maintained at DC bus by comparing the  $V_{dc}$  reference and  $V_{dc}$  bus. In grid-connected mode, three-phase voltage  $V_{abc}$  is converted into  $V_\alpha, V_\beta$  by  $abc$  to  $\alpha\beta$  transformation, which gives the  $\omega t$  from the PLL. now  $V_\alpha, V_\beta$  is further converted into  $E_d, E_q$  by  $\alpha\beta$  to  $dq$  transformation. Current controller is used here and it is again converted into  $V_{abcref}$  which controls the inverter by PWM technique. LCL filter is used to suppress the total harmonic distortions. In grid-connected mode, single PID controller is used. Capacitor is used to maintain the constant DC voltage for the input of inverter. This controller is designed for the three-phase balanced load condition. Figure 7 shows inverter control for grid connected mode.

In island mode,  $\omega.t$  should be given from outside and two PID controller is used. One of them is current controller and the other is voltage controller.  $V_{abc}$  is converted into  $V_d, V_q$  by injecting the  $\omega t$  by  $abc$  to  $dq$  transformation. For the islanding mode, voltage reference is given which is denoted by  $V_{dref}$ .  $V_{qref}$  is set zero for the unity power factor. The voltage controller PID produced the  $I_{dref}$  and  $I_{qref}$  which is further used with  $I_d$  and  $I_q$ , and the error is minimized by using PID controller. Then, it is further transformed from  $dq$  to  $abc$  for the generation of inverter switch which is controlled by PWM technique.  $V_{qref}$  is set to zero for unity power factor mode. Figure 8 shows inverter control for islanding mode.

### 4.3 LCL filter Modeling and Design

Current ripple, filter size, and switching ripple attenuation are the significant restrictions to be considered while designing the LCL filters. The capacitor’s effect on the grid’s reactive power fluctuation may result in resonance, which might make the system run in an unsteady way. For passive or active dampening, it is advised to either change the controller design or put a resistor in series with the capacitor. A basic L-filter only has a 20 dB/decade attenuation over the full frequency range, making an LCL filter more effective. There are more losses as the switching frequency rises. Like the grid inductance, the resonance frequency of LC filters varies over time. As a result,

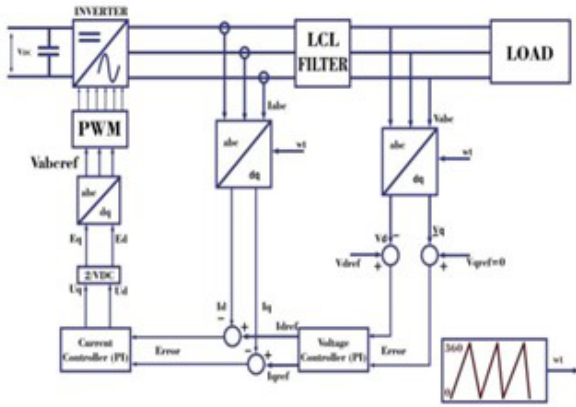


Figure 8: Inverter control for islanding mode

they are not suitable for a shaky grid. Figure 9 shows the flowchart of LCL filter.

#### 4.4 Design Procedure

The filter design technique has been presented thoroughly and the resonance difficulties can be mitigated passively or actively if properly damped. The inputs for determination of settings of LCL filter are power rating of the converter, frequency of the grid, and the switching frequency.

The greatest power factor fluctuation perceived by the grid is estimated to be 5% when the value of the system's base impedance is multiplied by  $C_f = 0.05C_b$  for the filter capacitance design. The maximum current ripple at the output of DC/AC inverter is given by Equation 6.

$$\Delta I_{max} = 2V_{DC}(1 - m)mT_{sw}/3L1 \quad (6)$$

, where m is the modulation factor.

The LCL filter's main objective is to minimize the anticipated 10 percent current ripple limit to 20 percent of its value, producing an output current ripple value of 2 percent.

### 5. Results and Discussion

Microgrid model is developed and simulated in MATLAB 2021Ra and simulated for 7 seconds

#### 5.1 PV Output

The output voltage obtained from the PV is in the range of 260 V to 275 V. Here, the output current is in the range of 78 A to 48 A. Due to the irradiance range of 1000 to 600  $W/m^2$ , MPPT is performed and the variable power is obtained in the range of  $1.3 \times 10^{-4}$  to  $2.1 \times 10^{-4}$ . The obtained result shows that the increase in irradiance results in increased voltage, current and power respectively. Wind power is changed corresponding to the change in wind speed. When the wind speed is changed, the current is changed. Here wind speed is changed in the range of 8-12 m/s and corresponding power is shown in the respective figure.

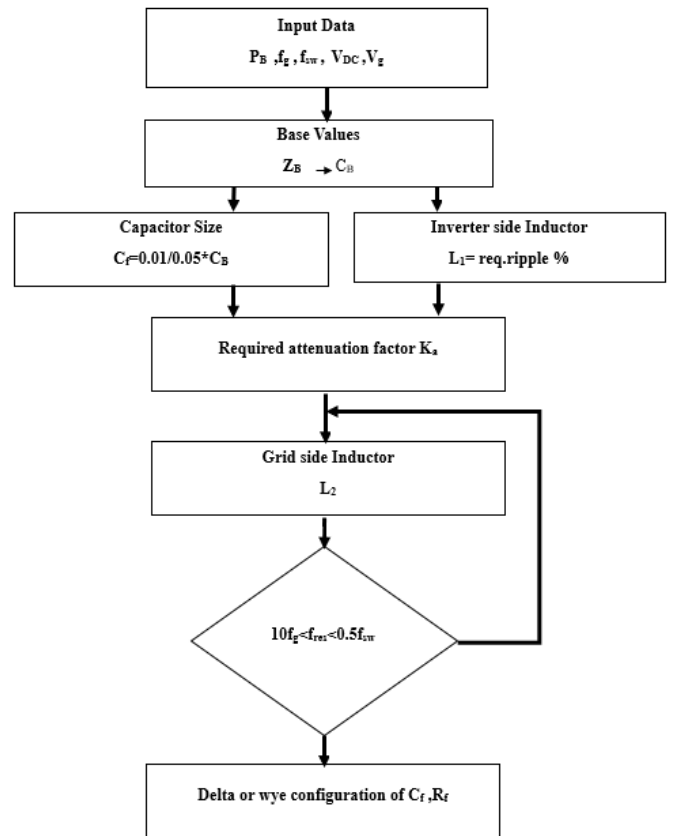


Figure 9: Flowchart of LCL filter

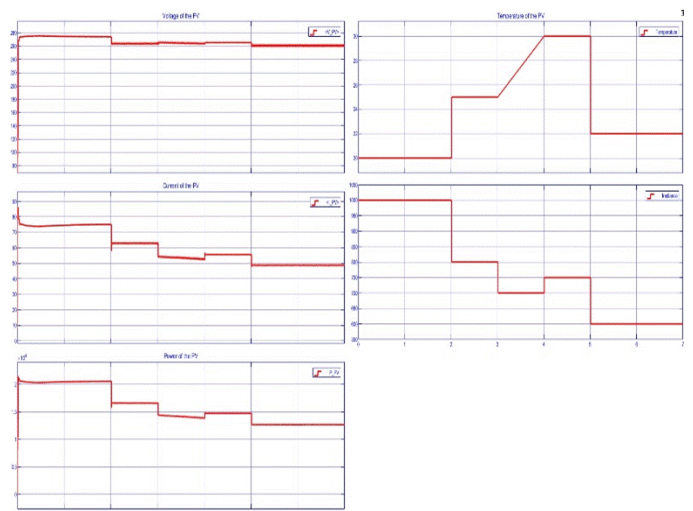


Figure 10: PV Output

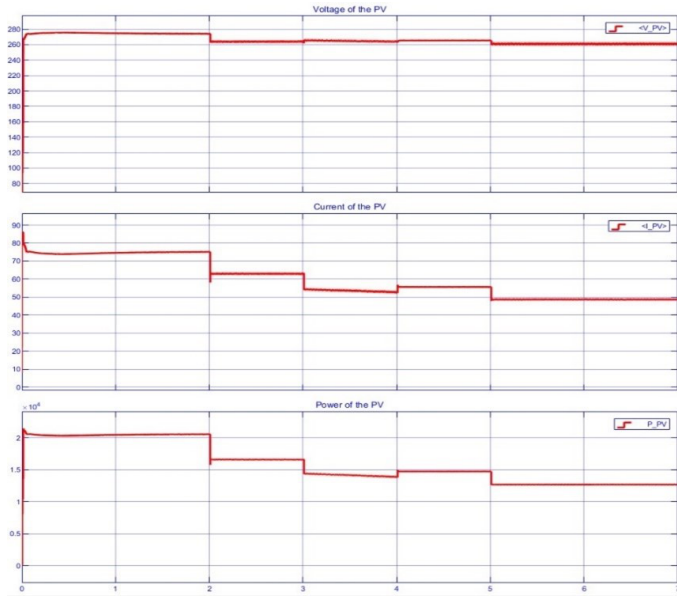


Figure 11: Microscopic view of PV Output (a)

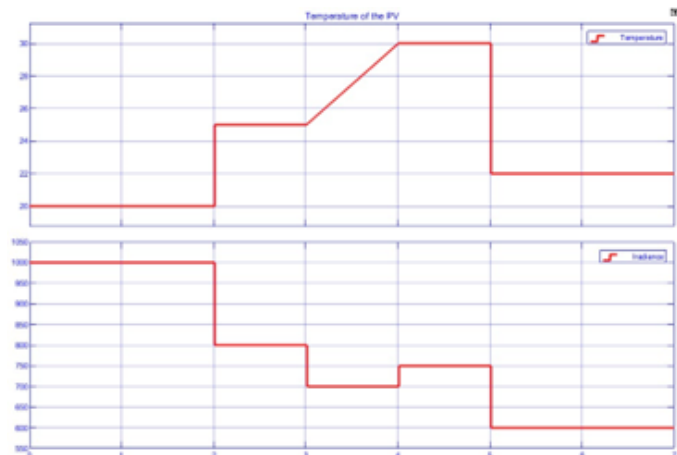


Figure 12: Microscopic view of PV Output (b)

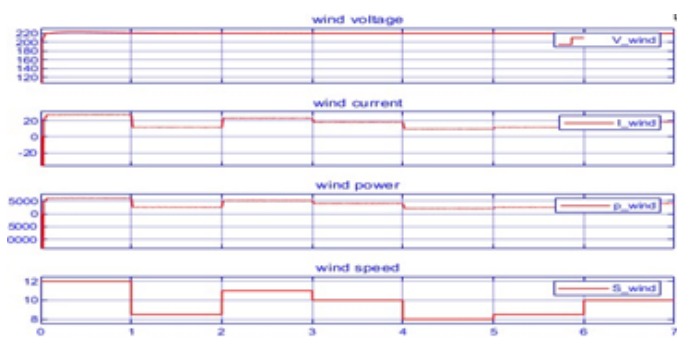


Figure 13: Wind Output

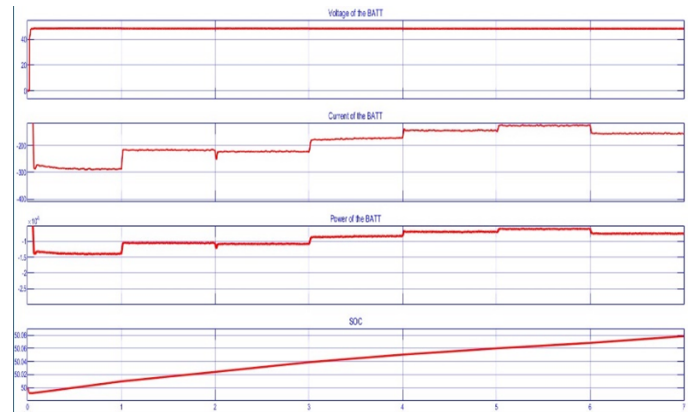


Figure 14: Battery Output

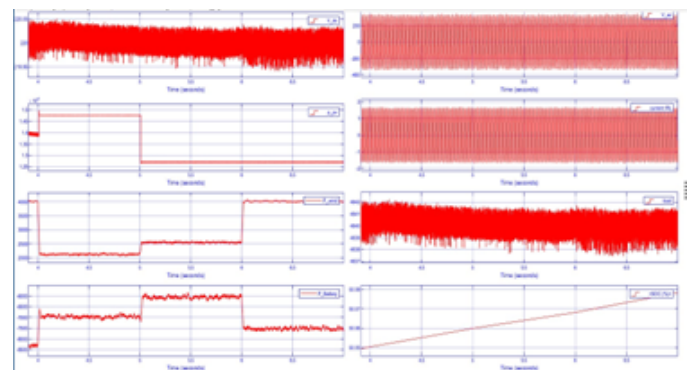


Figure 15: Grid forming mode

## 5.2 Battery Output

The voltage of the battery is 48 V. Buck-boost converter is used to regulate the DC voltage. The negative power in the battery signifies that the battery absorbs the power and the battery is charging. In islanding condition, when load is greater than generation, power is maintained by storage system. The positive power on battery shows that it delivers the power to the load and also signifies that the SOC of the battery is decreasing with time. This figure clearly elucidates that when the generation is high, the power supplied by the battery is low and it maintains the load power. When generation is low, the battery delivers the high power to maintain the power balance.

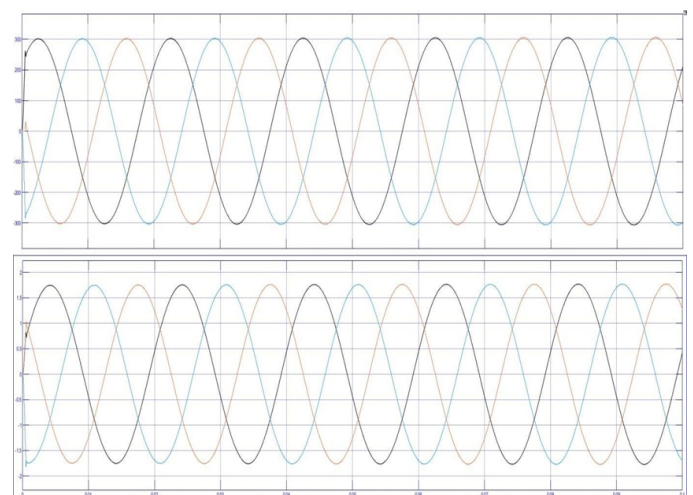


Figure 16: Output AC voltage and current waveform

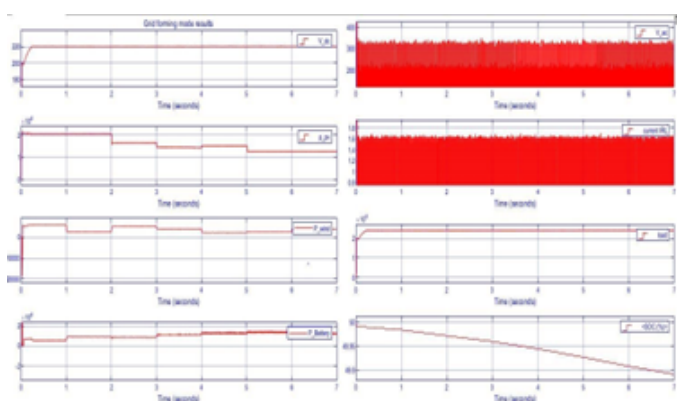


Figure 17: Islanding mode battery discharging condition

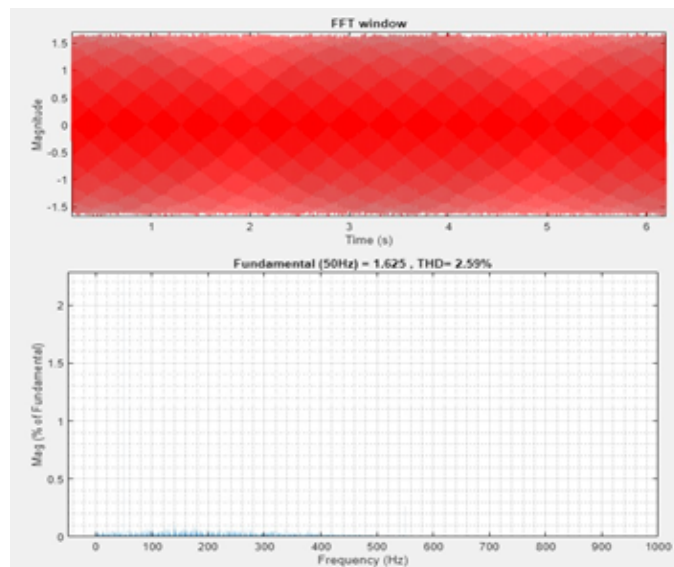


Figure 20: THD for Grid forming mode

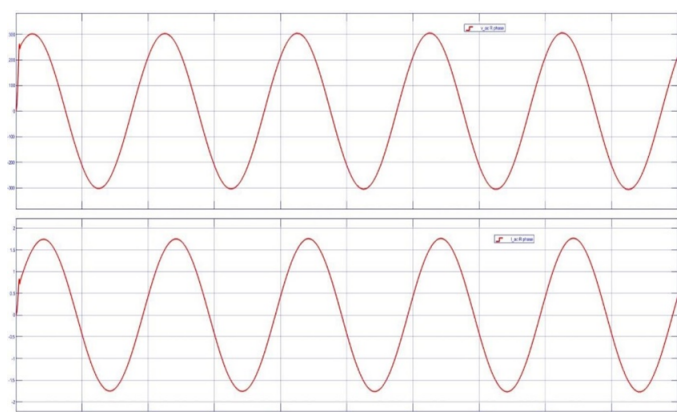


Figure 18: Output voltage and current waveform at load 1

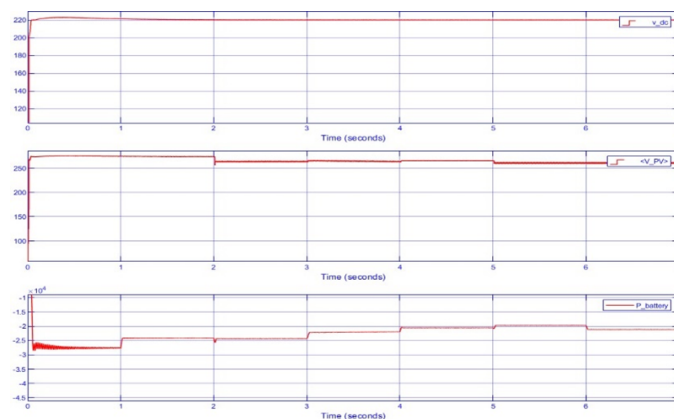


Figure 21: Battery output

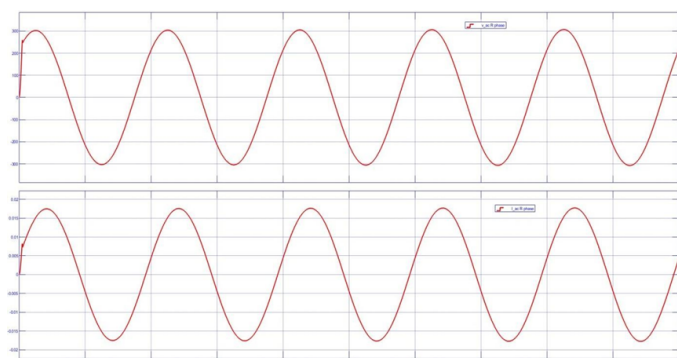


Figure 19: Output voltage and current waveform at load 2

In grid forming mode, the DC bus voltage is maintained at 220 V, which is fluctuating in the range of 119.6 V to 220.8 V with production and the load varies with time. The output of rms value of AC voltage is 200 V. The negative power in the battery shows that it absorbs the power and the SOC of the battery is increased. The battery is charged. The output voltage and current at two different load conditions are presented. In grid forming mode, total harmonic distortion (THD) was found to be 2.59% in current waveform, which is acceptable as per IEEE standard.

This is case where some amount of power is feeding to grid and battery is also getting charged. Negative power in the battery signifies that it absorbs the power. In charging conditions, the SOC of the battery increases with time. The battery SOC is found to be increased from 50 to 50.2 within 7 seconds. The DC bus voltage is maintained at 220 V.

In grid feeding condition, the reference frequency for the grid is 50 Hz. From the simulation, its value is fluctuating in the range of 49.80 Hz to 50.20 Hz due to the change in generations and load.

The grid voltage and current were found to be in phase and the three-phase voltage is found to be perfectly sinusoidal. 50 A current is feeding to the grid. In grid feeding mode, the total harmonic distortion was found to be 2.43% in voltage waveform,



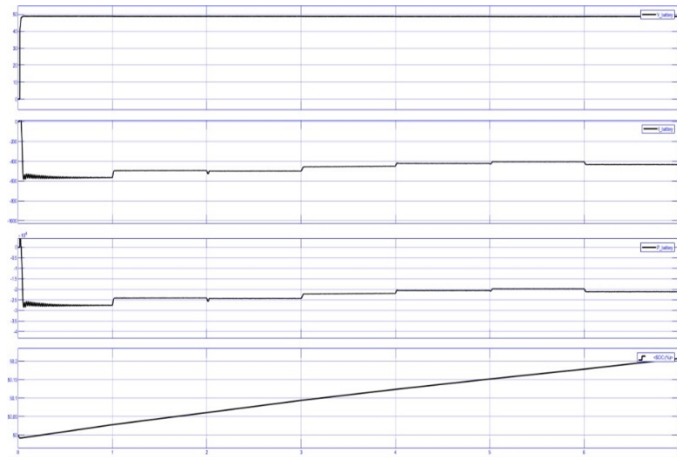


Figure 22: Detailed output when power is feeding to grid and battery charging mode

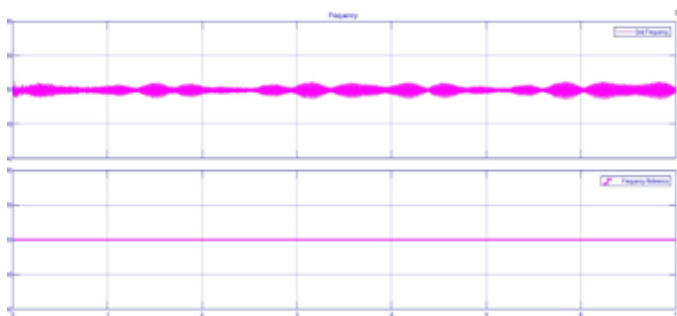


Figure 23: Frequency Output

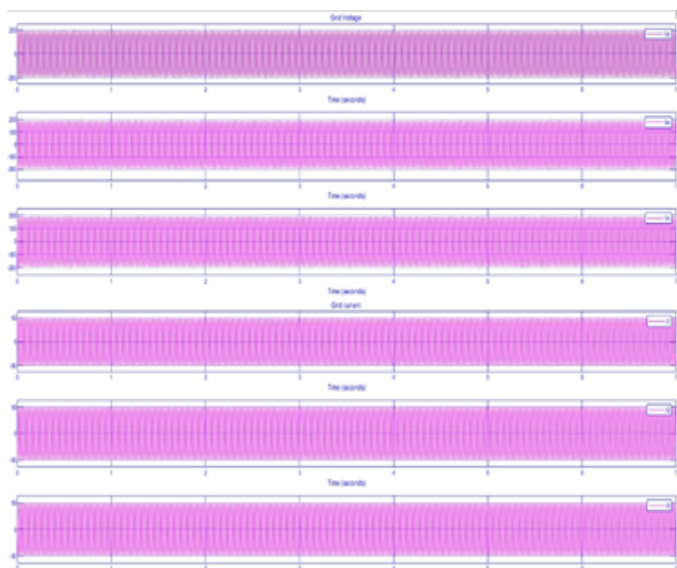


Figure 24: Grid voltage and current

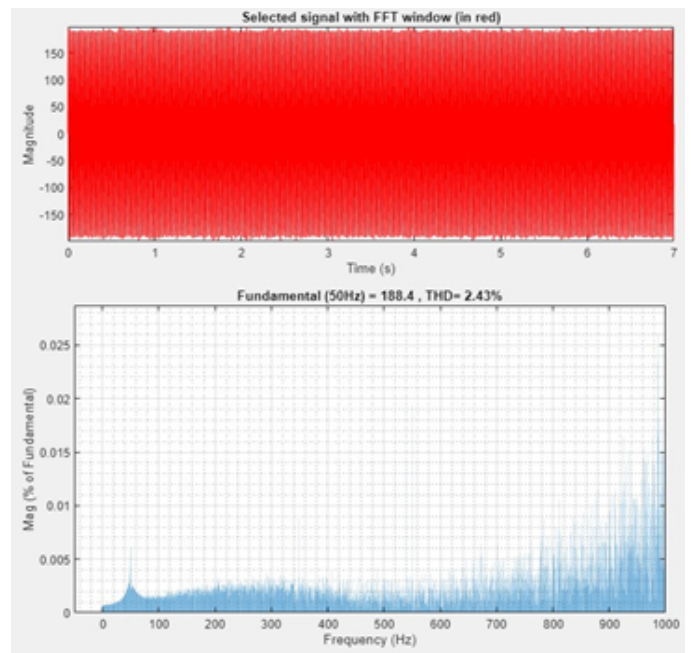


Figure 25: THD for grid current (a)

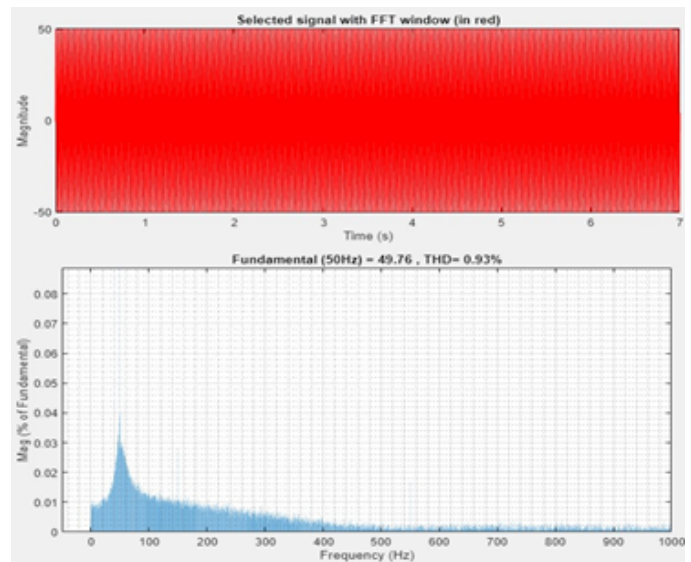


Figure 26: THD for grid current (b)

which is acceptable as per IEEE standard.

The total harmonic distortion (THD) was found to be 0.93% in current waveform.

## 6. Conclusion

This research shows the design of DC microgrid which is able to operate in both the grid feeding and grid forming mode. The result obtained from the simulation justifies the research and its overall aim. Although it will be a demanding challenge in the future, integrating decentralized energy generation, particularly intermittent sources like solar and wind energy, will be crucial. The difficulty lies in creating adaptable "Plug and Play"-based integration solutions for such sources into the network. The idea of microgrids with storage devices might be the solution to interconnection problems. As highlighted in the research paper, the integration of intermittent renewables and the self-

sustainability of such systems entail the usage of storage. The DC microgrids that are suggested have a battery storage system. The goal of this work was to create control algorithms that can guarantee the stability of DC microgrids even in the face of abrupt and significant changes in production and consumption.

Microgrid islanding mode is possible with satisfying power quality issue and stability perspective. Storage device is more important due to the fact that microgrids controllable DG sources have low inertia and slow ramp-up rates and in the case of uncontrollable DG sources for power balance operation. The perfect combination of inverter mode is necessary for the islanding operation. If there are no controllable micro sources in the microgrid, the storage devices will still inject power in the microgrid until their energy is consumed and blackout occurs. No single DG is suitable for microgrids.

## References

- [1] Baoquan Liu, Fang Zhuo, Yixin Zhu, and Hao Yi. System operation and energy management of a renewable energy-based dc micro-grid for high penetration depth application. *IEEE Transactions on Smart Grid*, 6(3):1147–1155, 2014.
- [2] Thilo Bocklisch. Hybrid energy storage systems for renewable energy applications. *Energy Procedia*, 73:103–111, 2015.
- [3] Iván Patrao, Emilio Figueres, Gabriel Garcerá, and Raúl González-Medina. Microgrid architectures for low voltage distributed generation. *Renewable and Sustainable Energy Reviews*, 43:415–424, 2015.
- [4] TM Kishorbha and DGP Mangroliya. Recent trades in distribution system. *International Journal of Advance Engineering and Research Development*, 2(3):211–217, 2015.
- [5] Dinesh Kumar, Firuz Zare, and Arindam Ghosh. Dc microgrid technology: system architectures, ac grid interfaces, grounding schemes, power quality, communication networks, applications, and standardizations aspects. *Ieee Access*, 5:12230–12256, 2017.
- [6] Quang Linh Lam. *Advanced control of microgrids for frequency and voltage stability: robust control co-design and real-time validation*. PhD thesis, Université Grenoble Alpes, 2018.
- [7] Sergio Vazquez, Srdjan M Lukic, Eduardo Galvan, Leopoldo G Franquelo, and Juan M Carrasco. Energy storage systems for transport and grid applications. *IEEE Transactions on industrial electronics*, 57(12):3881–3895, 2010.
- [8] Wei Sun, Zhe Chen, and Xiaojie Wu. Intelligent optimize design of lcl filter for three-phase voltage-source pwm rectifier. In *2009 IEEE 6th International Power Electronics and Motion Control Conference*, pages 970–974. IEEE, 2009.
- [9] Sergio Vazquez, Srdjan M Lukic, Eduardo Galvan, Leopoldo G Franquelo, and Juan M Carrasco. Energy storage systems for transport and grid applications. *IEEE Transactions on industrial electronics*, 57(12):3881–3895, 2010.
- [10] Andre Pires Nobrega Tahim, Daniel J Pagano, Eduardo Lenz, and Vinicius Stramosk. Modeling and stability analysis of islanded dc microgrids under droop control. *IEEE Transactions on power electronics*, 30(8):4597–4607, 2014.
- [11] TM Kishorbha and DGP Mangroliya. Recent trades in distribution system. *International Journal of Advance Engineering and Research Development*, 2(3):211–217, 2015.
- [12] Sabah Siad, Gilney Damm, Lilia Galai Dol, and Alexandre de Bernardinis. Design and control of a dc grid for railway stations. In *PCIM Europe 2017; International Exhibition and Conference for Power Electronics, Intelligent Motion, Renewable Energy and Energy Management*, pages 1–8. VDE, 2017.
- [13] Miguel Jiménez Carrizosa, Fernando Dorado Navas, Gilney Damm, and Françoise Lamnabhi-Lagarrigue. Optimal power flow in multi-terminal hvdc grids with offshore wind farms and storage devices. *International Journal of Electrical Power & Energy Systems*, 65:291–298, 2015.
- [14] Ahmed T Elsayed, Ahmed A Mohamed, and Osama A Mohammed. Dc microgrids and distribution systems: An overview. *Electric power systems research*, 119:407–417, 2015.
- [15] Dae Keun Yoo and Liuping Wang. A model predictive resonant controller for grid-connected voltage source converters. In *IECON 2011-37th Annual Conference of the IEEE Industrial Electronics Society*, pages 3082–3086. IEEE, 2011.
- [16] Lijun Gao, Shengyi Liu, and Roger A Dougal. Dynamic lithium-ion battery model for system simulation. *IEEE transactions on components and packaging technologies*, 25(3):495–505, 2002.
- [17] Sergio Vazquez, Srdjan M Lukic, Eduardo Galvan, Leopoldo G Franquelo, and Juan M Carrasco. Energy storage systems for transport and grid applications. *IEEE Transactions on industrial electronics*, 57(12):3881–3895, 2010.
- [18] Guannan Lou, Wei Gu, Wanxing Sheng, Xiaohui Song, and Fei Gao. Distributed model predictive secondary voltage control of islanded microgrids with feedback linearization. *IEEE Access*, 6:50169–50178, 2018.
- [19] Alessio Iovine, Sabah Benamane Siad, Gilney Damm, Elena De Santis, and Maria Domenica Di Benedetto. Nonlinear control of a dc microgrid for the integration of photovoltaic panels. *IEEE Transactions on automation science and engineering*, 14(2):524–535, 2017.